Chemical Engineering Journal 98 (2004) 89–97

Chemical Engineering Journal

www.elsevier.com/locate/cej

Determination of the gibbsite dehydration reaction pathway at conditions relevant to Bayer refineries

B. Whittington, D. Ilievski*

AJ Parker CRC for Hydrometallurgy, CSIRO Minerals, P.O. Box 90, Bentley, WA 6982, Australia

Accepted 12 July 2003

Abstract

The calcination of gibbsite to alumina is the last major step in the Bayer process. Despite its commercial importance, little attention has been given to determining the gibbsite thermal dehydration reaction pathway under conditions of relevance to this commercial process. Results from this study show that, at the temperatures and high heating rates relevant to the Bayer plants, gibbsite dehydrates mainly via chi alumina, which then reacts to gamma alumina, theta alumina and alpha alumina. Dehydration via boehmite is a minor reaction pathway. Experimental results are also presented that indicate chi alumina can react to gamma alumina at low heating rates.

It was shown that the phase compositions of different refinery smelter-grade aluminas, formed in fluid-bed calciners (FBCs), could be reproduced with laboratory-calcined aluminas by controlling the calcination time.

Keywords: Alpha alumina; Calcination; Chi alumina; Dehydration; Fluid-bed calciner; Gamma alumina; Gibbsite; Rotary-kiln calciner

1. Introduction

The Bayer process is used for the preparation of alumina from bauxite ore and is of considerable commercial importance. An important intermediate step is the drying and calcination of the gibbsite precipitate to smelter-grade alumina (SGA), in either a rotary-kiln calciner (RKC) or a fluid-bed calciner (FBC).

Reaction pathways for the dehydration of gibbsite are presented in Fig. 1. Wefers and Misra [14] report that the dehydration reaction pathways and kinetics are affected by heating rate, particle size and the water vapour pressure around the particle. It is generally accepted that dehydration of gibbsite via boehmite (Fig. 1b) is more likely to occur for larger gibbsite particles ($\geq$50 μm, e.g. [12,14]). Boehmite is not expected to form in small particles, as the water is able to escape without a significant increase in internal pressure. Refinery calciners contain significant water vapour, generated by the burning of fuel to provide heat and by the dehydration of gibbsite, and it is expected that under these conditions gibbsite dehydrates mainly via boehmite.

However, Ingram-Jones et al. [5] report an additional pathway (Fig. 1c) whereby gibbsite dehydrates via chi alumina and then to gamma alumina when subjected to high heating rates (4700–15,000 °C s^{-1}). Yamada et al. [19] report yet another pathway, in which gibbsite dehydrates predominately via chi alumina in a FBC (Fig. 2, main pathway). This chi alumina then reacts to pseudo-gamma alumina in a pathway similar to that of Ingram-Jones et al. [5]. However, Yamada et al. [19] did not detail how they characterised the materials, making it difficult to comment on the accuracy of their quantification methodology. As shall be shown, quantifying the so-called transition aluminas requires some care.

In this paper the gibbsite dehydration pathway, at conditions relevant to the alumina industry, was determined by studying accurate phase composition data obtained at different calcination times ranging from 8 s to 300 min. An XRD-based method was developed to quantify the phases present in various aluminas. This method simulates the XRD trace of the "unknown mixture" as the sum of the XRD traces of the various "pure-phase" materials (i.e. boehmite, gamma alumina, theta alumina, chi alumina, kappa alumina and alpha alumina). The parameters in the model, which include phase concentrations, peak width, 2θ offset and XRD correction factor, are determined by minimising the difference between the observed and calculated patterns. The accuracy and sensitivity of the method are demonstrated.

The relevance of the calcination procedure to the industrial scale will be considered by comparing the phase composition of the final (laboratory) product with that of SGA samples prepared using refinery (industrial-scale) calciners.

* Corresponding author.
E-mail address: dean.llievski@csiro.au (D. Ilievski).

1385-8947/$ – see front matter © 2003 Elsevier B.V. All rights reserved.
doi:10.1016/S1385-8947(03)00207-9

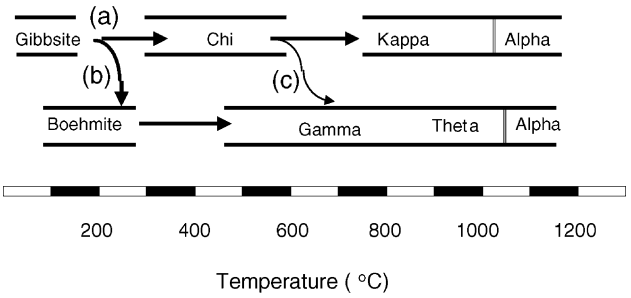

Fig. 1. Reaction pathways for gibbsite dehydration to alumina (modified from that in [14]). For calcination of small crystals (<10 μm) conducted in dry air (pressure 101 kPa) pathway (a) reportedly operates while calcination of large crystals (>100 μm) conducted in wet air at pressures in excess of 1 atm reportedly operates by pathway (b). Pathway (c) is reported to occur upon flash calcination of gibbsite [5].

2. Experimental procedure

2.1. Materials

A pseudo-radial gibbsite, similar in size and morphology to that found in the Bayer plants, was used in the calcination studies. A scanning electron microscope image of a "typical" gibbsite grain is shown in Fig. 3. The median particle size of this material is 91 μm, on a volume basis.

Refinery SGA samples were obtained from various refineries around the world operating either rotary-kiln or fluidised bed calciners.

2.2. Laboratory calcinations

Laboratory calcinations were conducted in a muffle furnace. Two nickel crucibles, each containing 1 g of gibbsite, were placed directly in the furnace at 970 °C. The furnace door was closed (time $t = 0$) and the timer started (approximately 3 s after $t = 0$—this time discrepancy was accounted for in all runs). The crucibles were removed from the furnace at specific times (taking into account the time required to remove the crucibles from the furnace) and the contents placed into a ceramic bowl. The bowl was then placed into a desiccator and the contents cooled (approximately 5 min) before transferring the alumina to a sample vial. Calcinations were conducted for times between 8 s and 300 min and each run was conducted in duplicate.

The laboratory procedure is not intended to be a small-scale physico-chemical model to simulate a refinery calciner. There was no direct control of the water vapour pressure or heating rate. However, by using a small quantity of gibbsite, in a small nickel crucible, it was possible to achieve the rapid heating rates found to be necessary to simulate the calcination process chemistry.

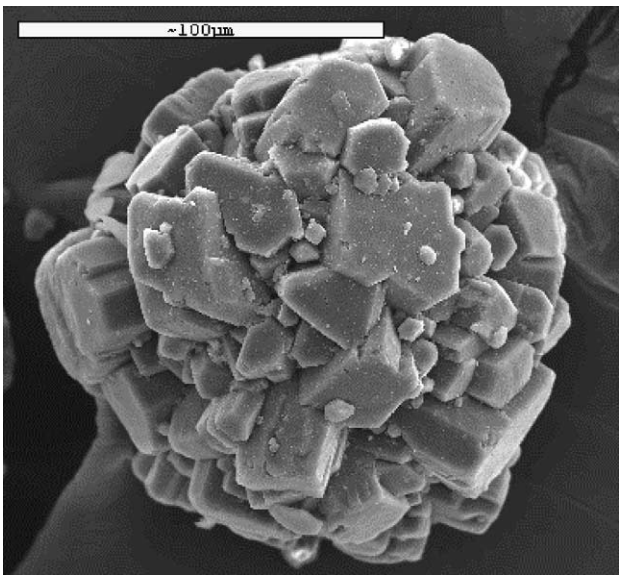

Fig. 3. SEM image of gibbsite used in this study.

2.3. Phase quantification

XRD traces of the powdered samples (ground for 2 min in a Glenn Creston ball mill) were obtained on a Philips "XPERT" series diffractometer that operated at 30 mA and 40 kV and used Co Kα radiation. Scans were obtained over the 2θ range 5–90° with a step size of 0.02° 2θ and 1 s per step. XRD traces of the external standard alumina samples were obtained in the same way within the same batch.

Quantitative analysis of the XRD trace used in-house software, which models the contribution of the boehmite, and the chi, gamma, theta, kappa and alpha alumina phases to the XRD trace and estimates the concentration of each phase in the alumina.

Pure-phase aluminas, or mixtures containing known amounts of impurities, were prepared by a number of methods (e.g. [1,11,17,20]). XRD traces were obtained of each material and the pattern of the phase of interest determined from this. The intensity of the XRD trace of a single alumina component was simulated as the combination of a number of Lorentzian peaks. The peak areas/widths and centroids were obtained from the XRD traces of the phase of interest.

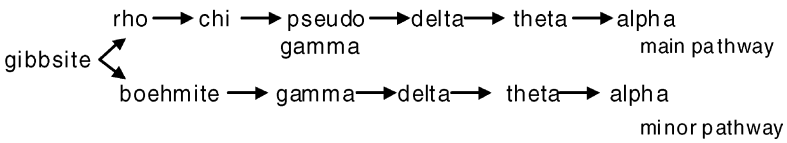

Fig. 2. Alternate gibbsite dehydration pathway proposed by Yamada et al. [19] for dehydration of gibbsite in a FBC.

Changes to the peak widths account for changes in the size of the diffracting domain, while changes to the XRD correction factor account for changes to the diffractometer tube output (i.e. changes in the integrated XRD peak intensity due to changes in the X-ray output). For a specific phase, the contribution of that phase to the XRD trace was obtained by summing the contributions of each major reflection from that phase that occurred between $2\theta = 5^\circ$ and 90°.

The concentration of alpha alumina in an alumina sample was also determined from the intensity of the alpha alumina (0 1 2) peak (3.48 Å) in the XRD trace relative to that of a pure alpha alumina standard [1]. The XRD traces were obtained over the 2θ range 27–33° using Co Kα radiation, 0.02° 2θ per step, 2 s per step.

2.4. Method validation

The accuracy of this technique was checked using synthetic mixtures of pure alumina phases made up to a known composition. The results in Fig. 4 indicate good agreement between the calculated and observed phase compositions.

The sensitivity of the calculated phase concentrations to the software parameters was determined by deliberate variations on the XRD correction factor, and the relative peak widths of the theta and alpha alumina. The effects are illustrated in Fig. 5.

It is possible to obtain accurate values for most of these software parameters and they will therefore have minimal

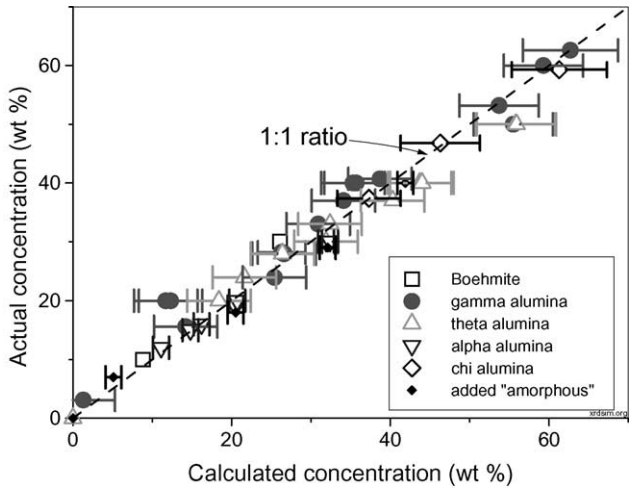

Fig. 4. Concentrations of boehmite, gamma alumina, chi alumina, theta alumina, alpha alumina and an amorphous material (fumed silica) calculated from the XRD profiles, compared with the actual concentrations.

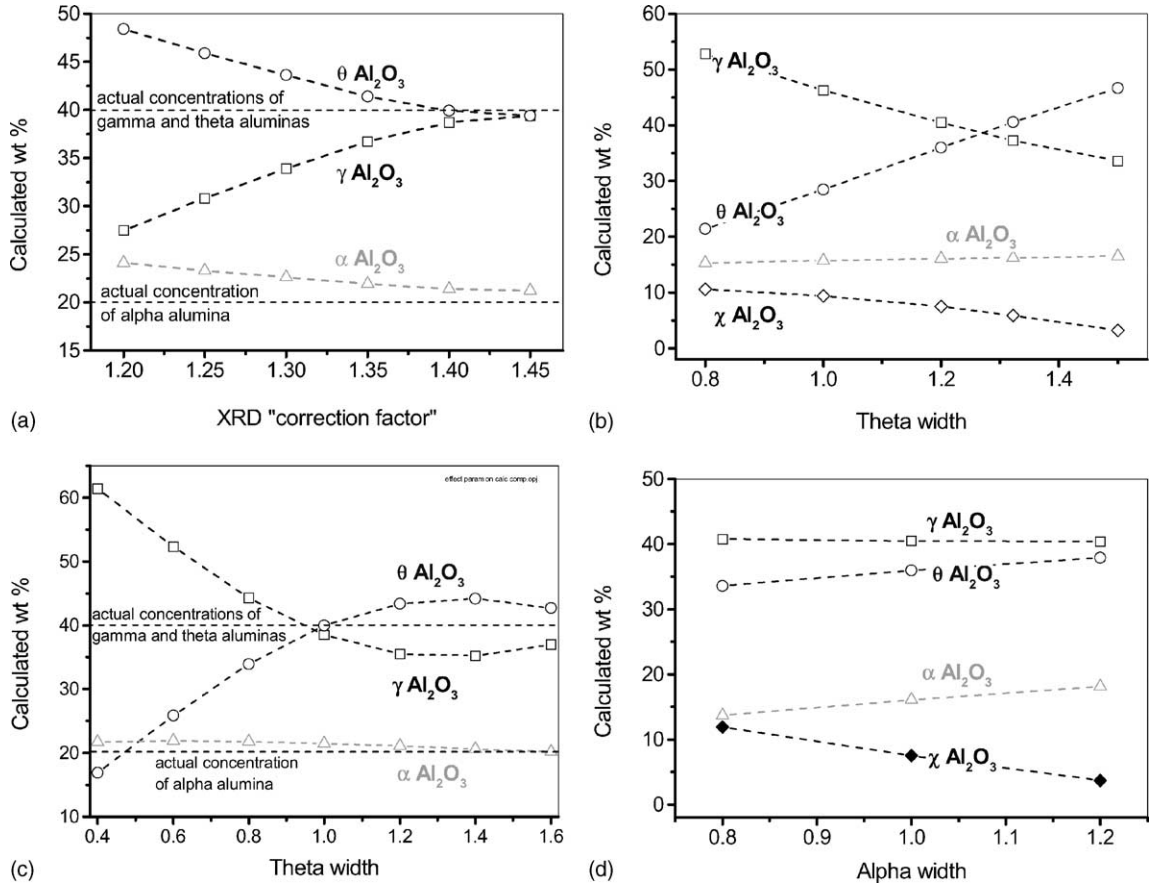

Fig. 5. Influence of changes to: (a) the XRD correction factor, (b) and (c) theta alumina peak width and (d) alpha alumina peak width on the calculated phase composition. The sample used to obtain this data was the gibbsite heated at 970 °C for 300 min that forms part of this overall study ((b) and (d)) or a synthetic standard ((a) and (c)).

impact on the calculated phase compositions. However, it is difficult to determine the relative theta alumina peak width in any sample, yet this parameter can influence the calculated concentrations of chi, gamma and theta aluminas (Fig. 5b). Note, however, that theta alumina peak width can affect the calculated phase composition only if samples contain greater than ~20% theta alumina and unrealistic theta alumina width values are used in the refinement (Fig. 5b and c; the theta alumina width values should be ≥1 for the samples examined in this paper). The theta width parameter will not, therefore, affect the calculated phase composition for the initial stages of the gibbsite dehydration.

A limitation of the method is that it does not allow for any variation in the XRD traces from those of the pure-phase standards used. Thus, it is unable to accommodate changes in the crystal structure occurring between samples, such as changes in the degree of preferred orientation or changes in crystal structure with temperature. The latter could be important if gamma alumina transforms to theta alumina in a displacement mechanism, in which the pores in gamma alumina merge to reduce the stacking faults (as suggested by Zhou and Snyder [20]). In this mechanism, a gradual sharpening and splitting of the diffraction pattern would be expected, which cannot be modelled using this current technique.

The current method, however, avoids the need for accurate crystallographic models—the absence of a reliable crystal structure for chi alumina severely limits the use of Rietveld refinement of the XRD trace for quantifying chi alumina/gamma alumina mixtures. The current method also avoids the difficulties in modelling peak anisotropy (i.e. variation in peak widths with (*h k l*) value).

3. Dehydration of gibbsite at 970 °C

3.1. Determination of gibbsite dehydration pathway

The measured phase compositions at various times over the first few minutes of calcination at 970 °C are shown in Fig. 6. The results in this figure indicate that gibbsite reacts to boehmite and these two phases are present for 8, 12, 15 or 22 s. Phases other than gibbsite or boehmite account for 24 or 57% of the total materials present in samples after 15 or 22 s, respectively. This unaccounted—for material may consist of poorly crystalline chi or rho aluminas—it is difficult to accurately identify these materials when present with gibbsite.

The sample calcined at 970 °C for 30 s consists mainly of chi alumina, with some boehmite and gamma alumina. The concentration of chi alumina decreases with increasing calcination time while the concentrations of gamma and theta aluminas increase (Fig. 6).

The results in Fig. 6 indicate some gibbsite reacts to boehmite, which then reacts to gamma and theta aluminas. However, even at the peak boehmite concentrations, less than

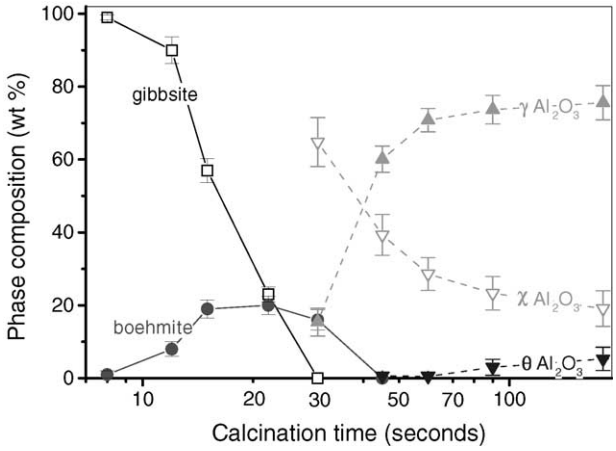

Fig. 6. Compositional changes upon laboratory calcination of gibbsite at 970 °C. Error bars refer to the maximum/minimum concentrations of each phase resulting from "errors" in the model parameters (i.e. calculated by deliberately varying the XRD correction factor (by ±0.05), boehmite peak width (by ±0.2) and theta alumina peak width (by ±0.2) from the "optimum" values, in a similar manner to that conducted in Fig. 5).

30% of the gibbsite is converted to boehmite. The majority of the gibbsite reacts via chi alumina and subsequently to gamma and theta aluminas in a pathway similar to that proposed by Ingram-Jones et al. [5]; see pathway c in Fig. 1. There are some similarities with the pathway proposed by Yamada et al. [19], namely that chi alumina transforms to gamma (pseudo-gamma) alumina. However, due to its very poor crystallinity it is difficult to determine if the rho alumina that Yamada et al. propose (see Fig. 2) forms during the initial dehydration stages at these conditions.

Results obtained at longer calcination times are shown in Fig. 7. These indicate that gamma alumina, forming either from the boehmite or the chi alumina, subsequently reacts to theta alumina (calcination times greater than 1 min) and then to alpha alumina (calcination times greater than 60 min). Minimal kappa alumina is present in these samples.

The presence of a diffraction peak occurring at ~2.1 Å (~50° 2θ Co Kα) is diagnostic of chi alumina [8,14]. The presence of a pronounced "hump" in the XRD trace of gibbsite calcined for 30 s (Fig. 8a), at ≈50° 2θ Co Kα, therefore supports the presence of significant chi alumina in this sample.

An alternative—although unlikely—reaction pathway is that gibbsite dehydrates via boehmite, and then via a "distorted" gamma alumina, and that it is this phase which fortuitously generates the peak in the XRD trace at ≈50° 2θ Co Kα. In the unlikely event that such a phase were to form, it should form from gibbsite or boehmite, especially since formation of such a phase from gibbsite would require gibbsite to react via boehmite. Since the XRD traces of boehmite calcined at 970 °C for 30 or 45 s contain no significant peak at ≈50° 2θ Co Kα (Fig. 8b and c), it is unlikely that the pronounced hump at ≈50° 2θ Co Kα (Fig. 8a) arises from anything other than chi alumina.

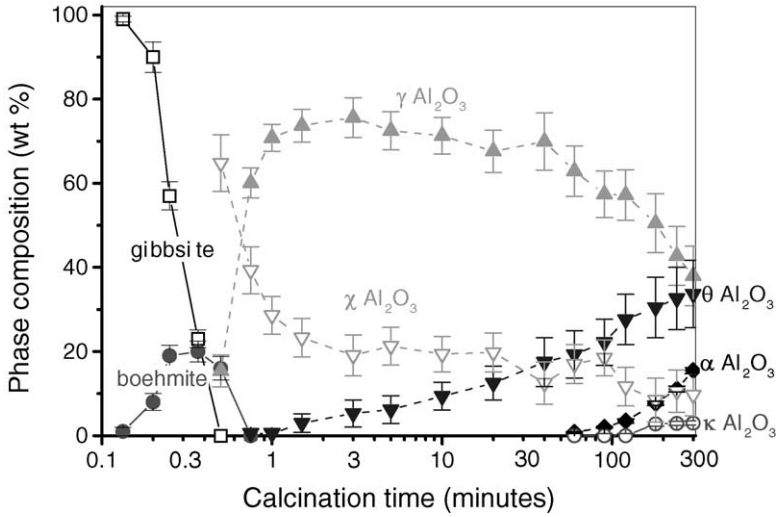

Fig. 7. Phases forming upon laboratory calcination of gibbsite at 970 °C and for the times shown. Details are the same as for Fig. 6.

3.2. Sizes of the diffracting domains in the various phases

Approximate crystallite sizes, or sizes of the ordering domains, of boehmite, gamma alumina and alpha alumina were determined by the application of the Scherrer formula

$$\text{crystallite size} = \frac{0.9\lambda}{\beta \cos\theta},$$

where λ is the diffraction wavelength, θ the Bragg diffraction angle and β the pure diffraction breadth; see [7] for more detail. β may be obtained from the observed width of the diffraction profile and the breadth of a line produced under similar diffractometer conditions using a sample that has no size, defect or strain broadening. A National Institute of Standards and Technology (NIST) standard reference material SRM 660, lanthanum hexaboride, was used in this study and the procedure outlined in [7] used to determine β. The boehmite (0 2 0), (1 2 0) and (0 3 1) peaks, and the alpha alumina (0 1 2), (1 0 4), (1 1 3), (0 2 4) and (1 1 6) peaks were used in the determination of crystallite sizes for these materials. Gamma alumina contains a number of overlapping peaks and the widths of the (2 2 0), (3 1 1) and (2 2 2) peaks were obtained by deconvoluting a Lorentzian profile.

The diffraction peaks of the initial gibbsite sample display mild anisotropy and the widths suggest diffracting domains larger than 600 nm for the {0 0 l} reflections and larger than 100 nm for the other ($h\,k\,l$) reflections. However, the SEM image in Fig. 3 suggests large crystallites and it is uncertain if these XRD-derived values are real or artefacts resulting from the limitations in the accuracy of the XRD determination for large crystallites.

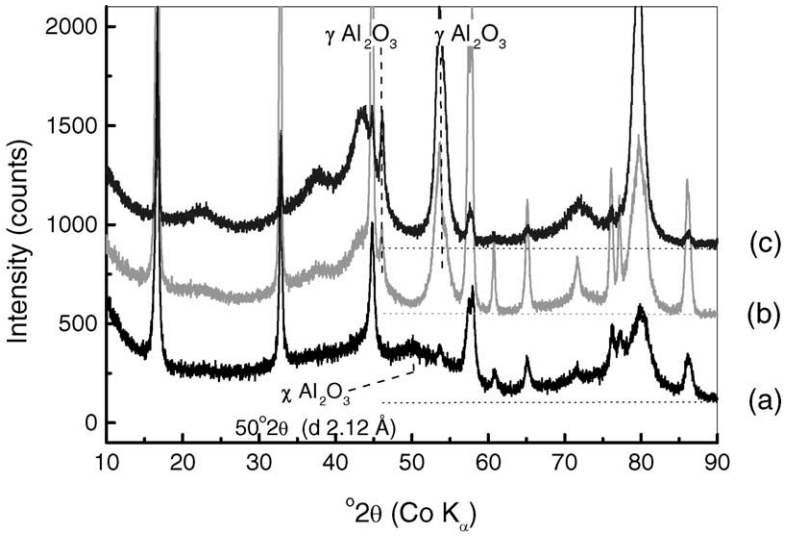

Fig. 8. XRD traces of materials formed upon laboratory calcination at 970 °C: (a) gibbsite heated at 970 °C for 30 s. Pure boehmite heated at 970 °C for: (b) 30 s and (c) 45 s.

The crystallite sizes of boehmite, present in the samples obtained after 12, 15 or 22 s calcination, are estimated to be (22 ± 5) nm and do not vary with (*h k l*) reflection or calcination time.

The gamma alumina displays significant peak anisotropy and the crystallite sizes estimated for the (2 2 0) and (3 1 1) peaks are significantly smaller than that estimated for the (2 2 2) peak: (2 ± 0.3) nm versus (25 ± 4) nm, respectively. The (2 2 2) and (2 2 0) reflections are dominated by scattering from the oxygen sublattice and the tetrahedral aluminium sublattices, respectively, and the crystallite sizes are consistent with the relatively ordered oxygen sublattice, but very disordered tetrahedral aluminium sublattice, proposed by Zhou and Snyder [20].

The peaks from the alpha alumina, which do not appear to vary with (*h k l*) reflection or sample calcination time (60–300 min), are consistent with crystallite sizes of (90 ± 30) nm.

4. Relevance Bayer refinery calcination

It was not possible to obtain Bayer refinery aluminous materials that had been calcined for the short time periods (∼30 s) necessary to elucidate the gibbsite dehydration pathway operating in commercial calciner systems. However, it was postulated that if alumina prepared in the laboratory furnace is of the same phase composition as the industrial SGA, then it is reasonable to assume that both formed by a similar dehydration reaction pathway.

Fig. 9a attempts to match the phase compositions of SGA formed in refinery FBCs with those of laboratory-calcined, corresponding refinery gibbsite. For each refinery SGA sample, calcined in a FBC, it is possible to obtain a laboratory-calcined alumina with a similar phase composition (Fig. 9a) by selecting a suitable calcination time. The main discrepancy between the two sets of data is in the relative concentrations of chi and gamma aluminas. It is possible to alter the phase compositions of the laboratory samples by altering parameters such as the heating rate and calcination time. However, it is not realistic to expect a perfect match between the laboratory samples that are prepared batch-wise and the industrial samples that are prepared in continuous flow systems with undefined particle residence time distributions.

The similarities in the phase composition of the numerous laboratory- and refinery-prepared aluminas suggest—but do not prove—that the majority of the refinery SGA forms via the chi alumina pathway.

The phase compositions of some refinery SGAs, prepared in a RKC, are shown in Fig. 9b, where they overlay the laboratory alumina with the same theta concentration. In contrast to the FBC SGA results, there is no apparent match between the composition of the refinery RKC SGA and that of laboratory-prepared alumina. This may be due to the relatively complex residence time distribution in the RKCs.

5. Gibbsite dehydration mechanism

5.1. Dehydration of gibbsite to boehmite

It is generally accepted (e.g. [12]) that hydrothermal conditions favour formation of boehmite from gibbsite. This has led to the hypothesis that boehmite forms in the hydrothermal conditions expected to occur at the centre of gibbsite particles. Rouquerol et al. [12] suggest that the presence of a gibbsite “shell” hinders the escape of excess water. Formation of boehmite reportedly stops when the intracrystalline pressure lowers due to crack formation [3,12] or thinning of the gibbsite shell [12].

Candela and Perlmutter [2] examine the dehydration of gibbsite to boehmite at 175–205 °C. The key features of their model are: (i) gibbsite dehydrates to boehmite with

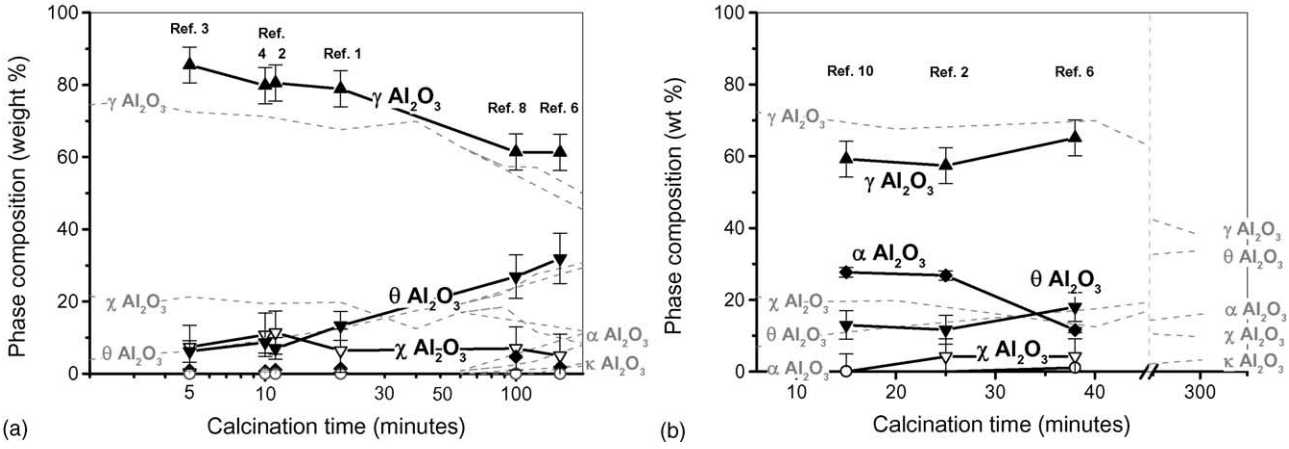

Fig. 9. Comparison of the phase composition of refinery SGA (solid lines) and alumina prepared by calcining gibbsite at 970 °C (dashed lines). (a) is for refinery SGA prepared in a FBC while (b) is for refinery SGA prepared in a RKC. The labels above the data points indicate the refinery from which the SGA samples were taken.

generation of porosity and escape of water product to the particle surface; (ii) dehydration of further gibbsite allows for growth of these boehmite nuclei; and (iii) growth of boehmite nuclei halts when the pores connecting various boehmite nuclei become accessible to the particle surface.

It is uncertain how, or where, gibbsite dehydrates to boehmite in the laboratory system used in the current work. However, XRD data indicates a reduction in the crystallite sizes in going from gibbsite to boehmite, but that there is no significant variation in boehmite crystallite size for calcination times between 8 and 30 s. This suggests that the boehmite nuclei grow rapidly to the average crystallite size of (22 ± 5) nm.

Candela and Perlmutter [2] indicate that the reaction of the remaining gibbsite (i.e. ~85%) occurs at a slower rate. They reported that the majority of the initially nucleated boehmite growth zones in the gibbsite particles are no longer "active" after 38% relative conversion to boehmite. The reduction in gibbsite dehydration rate could result from the deactivation of the boehmite nuclei through their being accessible to the surface. It is uncertain whether this reduction in gibbsite dehydration rate kinetically favours formation of chi alumina, or if other factors are responsible for the formation of this phase under the conditions used in this study.

5.2. Reaction of boehmite to gamma, theta and alpha aluminas

Wilson [16] proposes that the dehydration of boehmite is controlled by a diffusion process acting perpendicular to the pores. In this process, protons are lost from between the boehmite layers and the resulting interlayer sites are occupied by counterdiffusing Al cations. Such a mechanism is consistent with the proposal of Zhou and Snyder [20] that the ordered oxygen sublattice remains intact during dehydration of boehmite to transition aluminas.

The observation of a fine, lamellar $(0\,0\,1)_\gamma$ pore system in gamma alumina is consistent with the mechanism proposed by Wilson [16]. The slit-shaped pores in gamma alumina prepared by dehydration of boehmite are ~0.8 nm wide [16] while the pores forming upon dehydration of gibbsite are reportedly ~2–3 nm thick [14]. However, it should be noted that the pore dimensions of the pore system depend on the calcination conditions, e.g. water vapour pressure, and also possibly on starting material.

Zhou and Snyder [20] report gamma alumina, prepared from boehmite, displays increasing tetragonal deformation and ultimately react to theta alumina upon heating at 1000 °C.

These results, and the gradual sharpening and splitting of the diffraction patterns as gamma alumina transforms to theta alumina reported by Zhou and Snyder [20], suggest gamma alumina undergoes a displacive transformation to theta alumina and not a reconstructive transformation. In the former, the gamma alumina pores merge to reduce the stacking faults while in the latter, gamma alumina coexists with theta alumina. Examination of the XRD traces from samples studied in this work indicate a gradual change in the peak intensities/widths with increasing reaction time, also suggesting that gamma alumina undergoes a displacive transformation to theta. However, further work is required to confirm this.

Levin et al. [9] suggest the oxygen sublattice is generally unaffected by the gamma to theta alumina transformation and that the primary changes occurring in the gamma to theta transformation result from a redistribution of the aluminium cations. This redistribution also increases the pore diameter and decreases the resultant surface area [18].

Wen and Yen [15] report that theta alumina crystallites, of maximum size ~20 nm, initially transform to alpha alumina crystallites of ~17 nm size and that this occurs when the solid contains ~5% alpha alumina. These alpha alumina nuclei then rapidly grow to alpha alumina crystallites of 45–55 nm in size. There is no evidence to suggest such a mechanism operates in our laboratory system, since the alpha alumina has crystallite sizes of (90 ± 30) nm for alpha alumina contents greater than 0.8 wt.% (i.e. reaction times of 60 min or greater).

Kao and Wei [6] studied the transformation of theta alumina to alpha alumina in the presence of alpha alumina seed. They suggest the oxygen atoms "diffuse from the theta matrix across the boundary during transformation to alpha phase, and they generate vacancy clusters on the theta–alpha interface". Kao and Wei suggest diffusion of oxygen atoms in the alumina lattice should be the mechanism controlling the theta to alpha transformation.

5.3. Dehydration of gibbsite to chi alumina

Kogure [8] studied dehydration of gibbsite in a transmission electron microscope (TEM) electron beam and reported that chi alumina formed as the gibbsite layers shift laterally, moving slightly closer to each other to form a random close-packed arrangement of anions. The conditions in a TEM are different to those in a refinery calciner, but do allow for rapid heating of the gibbsite.

5.4. Reactions of chi alumina

The majority of references indicate that chi alumina reacts via kappa alumina (e.g. [4,14], and references therein; [10,13]). However, the conditions used in these studies are very different to those used in this study and also those in the refinery calciners, e.g. Gan [4] used a slow heating rate of 1 °C min^{-1}; Mardilovich et al. [10] calcined for 5 h at various temperatures.

When gibbsite is subjected to high heating rates, typically 4700–15,000 °C s^{-1}, then there is evidence that chi alumina reacts to gamma alumina [5]. Yamada et al. [19] report chi alumina reacts to pseudo-gamma alumina in a FBC, while Kogure [8] reports chi alumina reacts to gamma or eta alumina in a TEM.

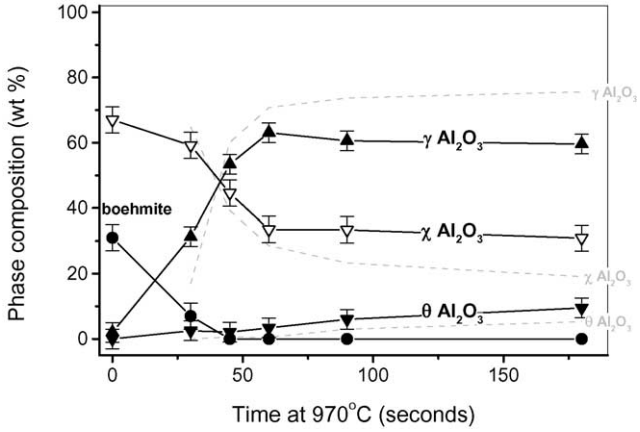

Fig. 10. Phases forming upon laboratory calcination, at 970 °C, of the aluminous material containing significant (66%) chi alumina (solid lines). Calcinations conducted using a heating regime similar to that employed in Figs. 6 and 7. Dashed lines indicate the change in composition of the chi, gamma and theta aluminas formed during the calcination of gibbsite (previously shown in Fig. 6).

Experiments conducted in this study examined the reaction of chi to gamma alumina by subjecting an aluminous material, containing significant (66%) chi alumina, to the same heating conditions as previously employed for the gibbsite. This material was prepared by heating gibbsite from room temperature to 400 °C at 0.5 °C min^{-1}. Boehmite is the other main phase present. The observed variation in phase composition of this material with calcination time is similar to that observed with the gibbsite, see Fig. 10, and supports the postulate that relatively high heating rates favour reaction of chi alumina to gamma alumina.

However, there is also evidence to suggest that chi alumina reacts to gamma alumina at lower heating rates. Although not explicitly stated by Gan [4], her data from the decomposition of Alcoa C33 gibbsite requires either that chi alumina reacts to gamma alumina or that the errors associated with the phase composition data are larger than those reported.

Further experiments using the chi alumina-rich material described above, confirmed that chi alumina can react to gamma alumina at relatively low heating rates. Heating this aluminous material from 400 to 700, at 0.5 °C min^{-1} results in a product consisting of 51% gamma alumina and 47% chi alumina. If no chi alumina had reacted to gamma alumina then heating the 32% boehmite/66% chi alumina starting material should have yielded a mixture containing 29% gamma alumina and 71% chi alumina.

In another experiment supporting the transformation of chi alumina to gamma alumina at a slow heating rate, a material consisting of 91% chi alumina and 9% boehmite, prepared by heating Alcoa Hydral gibbsite from room temperature to 400 °C at 0.5 °C min^{-1}, was heated from 400 to 700 °C at 0.5 °C min^{-1}. The product consisted of 33% gamma alumina and 67% chi alumina. The starting material should have yielded a mixture containing 8% gamma alumina/92% chi alumina if chi alumina did not react to gamma alumina. It is acknowledged that variations in the X-ray patterns of these gamma and chi aluminas from those of our "pure-phase standards" could affect the accuracy of the calculated phase concentrations. Nevertheless, these results do provide significant support for a chi alumina to gamma alumina transformation at both high and low heating rates.

6. Conclusions

The dehydration of a refinery gibbsite has been studied in a laboratory furnace at 970 °C. The variation in phase composition with time indicates that the majority (∼70%) of this gibbsite dehydrates via chi alumina and that significant concentrations of chi alumina react to gamma alumina, and then to theta and alpha aluminas. This mechanism is similar to that proposed by Ingram-Jones et al. [5] and displays some similarities with the pathway proposed by Yamada et al. [19], namely that chi alumina transforms to gamma (pseudo-gamma) alumina.

The phase composition was determined for a number of refinery SGA samples. For each refinery SGA sample, calcined in a FBC, it is possible to obtain a laboratory-calcined alumina with a similar phase composition. These similarities suggest—but do not prove—that the majority of the refinery SGA forms via the chi alumina pathway.

An aluminous material, containing significant (66%) chi alumina, and gibbsite were subjected to the same heating conditions and the variation in phase compositions with time were observed to be similar, confirming that relatively high heating rates favour the reaction of chi alumina to gamma alumina. Evidence was also presented showing that chi alumina can react to gamma alumina at lower heating rates.

Acknowledgements

Sincere thanks go to the industrial sponsors of the AMIRA P575 project for both their financial support and their active participation throughout the project, namely: Alcoa, Worsley Alumina, QAL, Comalco, Alcan Nabalco, Lurgi, Norsk Hydro, Billiton Aluminium, and Pechiney. Special thanks go to Steven Rosenberg of Worsley Alumina for his contributions to the project.

The authors gratefully acknowledge the support from the Australian Government's Cooperative Research Centre (CRC) program, through the AJ Parker CRC for Hydrometallurgy.

References

[1] Determination of alpha alumina content by X-ray diffraction, Australian Standard 2879, Part 3, Standards Australia, Sydney, NSW, Australia, 1991.

[2] L. Candela, D.D. Perlmutter, Kinetics of boehmite formation by thermal decomposition of gibbsite, Ind. Eng. Chem. Res. 31 (1992) 694–700.
[3] J.H. De Boer, J.M.H. Fortuin, J.J. Steggerda, The dehydration of alumina hydrates, Proc. Kon. Ned. Akad. Wetensch, Amsterdam B 57 (1953) 170–180.
[4] B.K. Gan, Crystallographic transformations involved in the decomposition of gibbsite to alpha alumina, Ph.D. Thesis, Curtin University of Technology, Australia, 1996.
[5] V.J. Ingram-Jones, R.C.T. Slade, T.W. Davies, J.C. Southern, S. Salvador, Dehydroxylation sequences of gibbsite and boehmite: study of differences between soak and flash calcination and of particle size effects, J. Mater. Chem. 6 (1996) 73–79.
[6] H.-C. Kao, W.-C. Wei, Kinetics and microstructural evolution of heterogeneous transformation of θ-alumina to α-alumina, J. Am. Ceram. Soc. 83 (2000) 362–368.
[7] H.P. Klug, L.E. Alexander, X-ray Diffraction Procedures for Polycrystalline and Amorphous Materials, Wiley, New York, 1962.
[8] T. Kogure, Dehydration sequence of gibbsite by electron-beam irradiation in a TEM, J. Am. Ceram. Soc. 82 (1999) 716–720.
[9] I. Levin, L.A. Bendersky, D.G. Brandon, M. Ruhle, Cubic to monoclinic phase transformations in alumina, Acta Mater. 45 (1997) 3659–3669.
[10] P.P. Mardilovich, A.I. Trokhimets, M.V. Zaretskii, G.G. Kupchenko, Spectroscopic investigation of dehydration of bayerite and hydrargillite, Zh. Prikl. Spektr. 42 (1985) 959–966.
[11] B. Ollivier, R. Retoux, P. Lacorre, D. Massiot, G. Ferey, Crystal structure of κ-alumina: an X-ray powder diffraction, TEM and NMR study, J. Mater. Chem. 7 (1997) 1049–1056.
[12] J. Rouquerol, F. Rouquerol, M. Ganteaume, Thermal decomposition of gibbsite under low pressures. I. Formation of boehmitic phase, J. Catal. 36 (1975) 99–110.
[13] M.-C. Stegman, D. Vivien, C. Mazieres, Etude du spectre infrarouge des alumines de transition et du corindon, J. Chim. Phys. 71 (1974) 761–764.
[14] K. Wefers, C. Misra, Oxides and hydroxides of aluminium, Alcoa Technical Paper No. 19, 1987 (revised).
[15] H.-L. Wen, F.-S. Yen, Growth characteristics of boehmite-derived ultrafine theta and alpha alumina particles during phase transformation, J. Cryst. Growth 208 (2000) 696–708.
[16] S.J. Wilson, The dehydration of boehmite, γ-AlOOH, to γ-Al_2O_3, J. Solid State Chem. 30 (1979) 247–255.
[17] S.J. Wilson, J.D.C. McConnell, A kinetic study of the system γ-Al_2O_3/Al_2O_3, J. Solid State Chem. 34 (1980) 315–322.
[18] S.J. Wilson, M.H. Stacey, The porosity of aluminium oxide phases derived from well crystallised boehmite: correlated electron microscope, adsorption and porosimetry studies, J. Colloid Interf. Sci. 82 (1981) 507–517.
[19] K. Yamada, T. Harato, S. Hamano, K. Horinouchi, Dehydration products of gibbsite in rotary kiln and stational calciner, Light Met. (1984) 157–171.
[20] R.-S. Zhou, R.L. Snyder, Structures and transformation mechanisms of the η, γ and θ transition aluminas, Acta Cryst. B47 (1991) 617–630.